ORGANOMETALLICS

ARTICLE

pubs.acs.org/Organometallics

Design, Synthesis, and Characterization of Functionalized Silepins: High Quantum Yield Blue Emitters

Lauren G. Mercier,[†] Shunsuke Furukawa,[‡] Warren E. Piers,*[,†] Atsushi Wakamiya,[§] Shigehiro Yamaguchi,[⊥] Masood Parvez,[†] Ross W. Harrington,[∥] and William Clegg[∥]

[†]Department of Chemistry, University of Calgary, 2500 University Drive NW, Calgary, AB, Canada T2N 1N4

[‡]Department of Chemistry, Graduate School of Science, University of Tokyo, 7-3-1 Hongo, Bunkyo-ku, Tokyo, Japan 113-0033

[§]Institute for Chemical Research, Kyoto University Uji, Kyoto, Japan 611-0011

[⊥]Department of Chemistry, Graduate School of Science, Nagoya University, Furo, Chikusa, Nagoya, Japan, 464-8602

[∥]School of Chemistry, Bedson Building, Newcastle University, Newcastle upon Tyne, U.K., NE1 7RU

Supporting Information

ABSTRACT: The synthesis of a family of 1,1-dimethyldibenzo[*b*,*f*]silepin derivatives, substituted with donor groups of various donor strength and conjugation length in the positions *meta* or *para* to the silepin silicon, is presented. The compounds were characterized by NMR, UV−vis, and fluorescence spectroscopy, as well as with cyclic voltammetry and DFT computations. One of the *meta* series was characterized by X-ray crystallography. All compounds show red-shifts in onset absorption and emission maxima compared to the parent 1,1-dimethyldibenzo[*b*,*f*]silepin, but all exhibit blue fluorescence with quantum yields ranging from 0.46 to 0.93 for the *meta* series and from 0.09 to 0.46 for the *para* derivatives. The data suggest that, for the *meta* series, the primary absorption is of $\pi-\pi^*$ character, while in the *para* series, for strongly donating groups, transitions from low-lying π orbitals to the LUMO+1 orbital, which has contributions from the C−Si−C σ^* orbitals, are charge-transfer in character. The phenyl-substituted derivatives can be converted to borepins via transmetalation with BBr_3, but other strategies are necessary to prepare borepins with other donor groups.

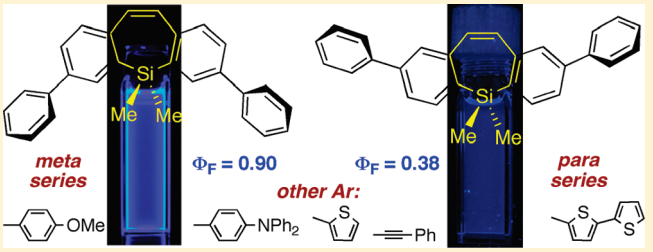

INTRODUCTION

Organic electronics comprises a large area of research, and many novel materials have been prepared that have applications in organic light-emitting diodes (OLEDs), organic field effect transistors (OFETs), and nonlinear optic materials (NLOs).[1−6] Organic electronics are generally poorer performing than inorganic materials in terms of electron transport, and lack of longterm stability can also detract from their use in certain applications. However, optoelectronic devices based on organic molecules and polymers have significant advantages over inorganic materials, including a wider array of processing options, cost effectiveness, and the ability to tune the photophysical properties of a class of molecules through synthesis and derivatization. Such modifications can lead to fine control over, for example, the HOMO−LUMO gap of the material, as well as the absolute energies of these frontier orbitals.

Perturbation of the HOMO−LUMO orbitals in π-conjugated molecules can be accomplished by modification of the material's basic structural framework and extension of conjugation by appropriate annulation or substitution patterns. Another strategy is to replace carbon atoms with heteratoms, such as silicon.[7] For example, 1,1-dialkyl siloles and substituted derivatives (**I**, Chart 1), silicon analogues of the fluorene framework, have been extensively studied and display strong fluorescence and good carrier mobilities.[8−26]

Chart 1

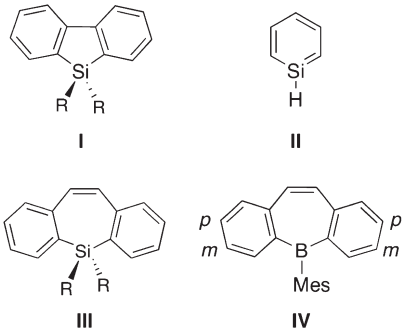

Absorption maxima are red-shifted compared to the all-carbon analogue fluorene, since the σ^* orbitals of the exocyclic Si-CH_3 groups interact with the π^* orbital of the butadiene fragment and lower LUMO energy.[17,27] Silabenzenes (**II**) also have interesting photoluminescence properties, but are less explored due to their more challenging synthesis and high reactivity.[28,29] Tokitoh utilized kinetic stabilization of the silabenzene

Received: January 21, 2011
Published: February 28, 2011

   dx.doi.org/10.1021/om2000597 | *Organometallics* 2011, 30, 1719–1729

Scheme 1

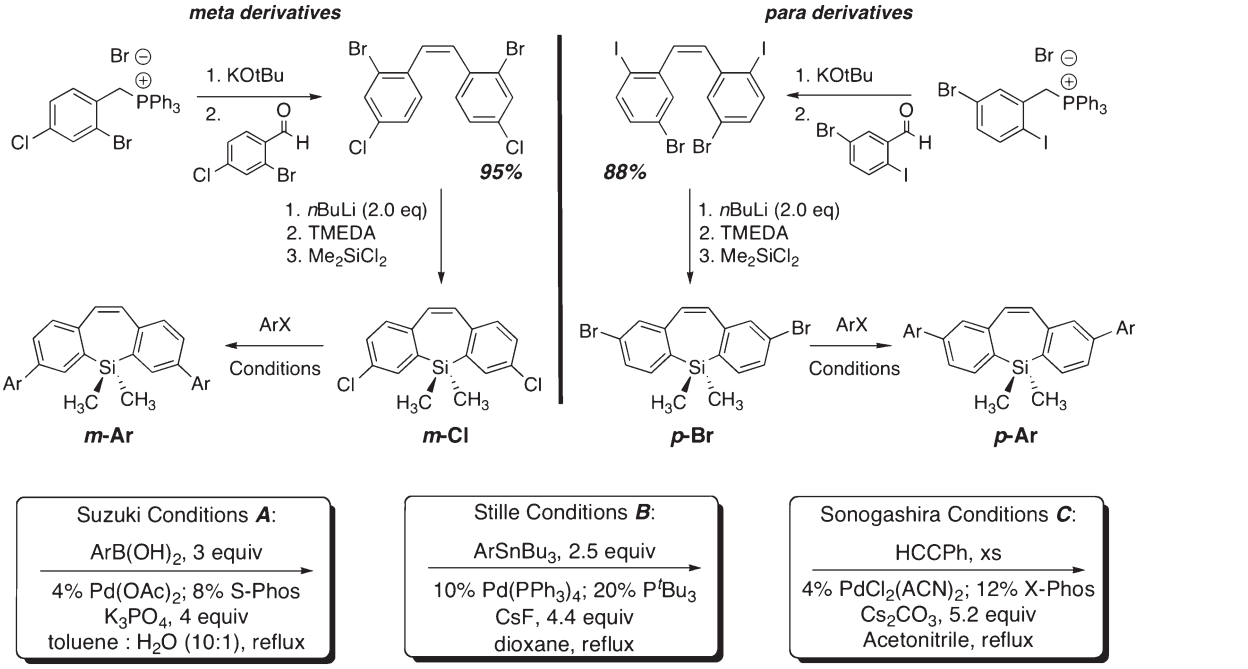

Table 1. Conditions and Yields of Suzuki, Stille, and Sonogashira Coupling Reactions

Compound	Ar	Conditions	*meta* Yields	*para* Yields
***m*/*p*-1-Ph**		**A**	65%	88%
***m*/*p*-1-PhOMe**	OMe	**A**	70%	95%
***m*/*p*-1-PhNPh$_2$**	NPh_2	**A**	84%	41%
***m*/*p*-1-Th**		**B**	66%	96%
***m*/*p*-1-bTh**		**B**	43%	52%
***m*/*p*-1-CCPh**	Ph	**C**	50%	43%

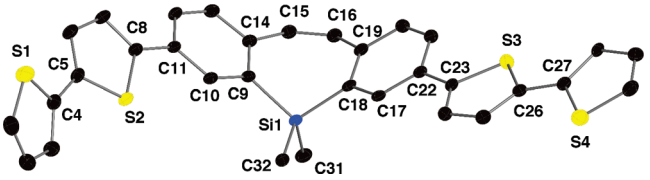

Figure 1. Displacement ellipsoid diagram (50% probability level) for the molecular structure of ***m*-1-bTh**. Selected bond distances (Å): Si(1)−C(9), 1.872(3); Si(1)−C(18), 1.874(3); Si(1)−C(31), 1.865(3); Si(1)−C(32), 1.860(3); C(9)−C(14), 1.404(4); C(14)−C(15), 1.470(4); C(15)−C(16), 1.343(4); C(16)−C(19), 1.475(4); C(18)−C(19), 1.413(4). Selected bond angles (deg): C(9)−Si(1)−C(18), 105.00(12); C(9)−Si(1)−C(31), 108.98(14); C(9)−Si(1)−C(32), 113.26(14); C(18)−Si(1)−C(31), 111.92(14); C(18)−Si(1)−C(32), 109.07(14); C(31)−Si(1)−C(32), 108.63(16); Si(1)−C(9)−C(14), 122.0(2); C(9)−C(14)−C(15), 124.2(3); C(14)−C(15)−C(16), 130.5(3); C(15)−C(16)−C(19), 132.3(3); C(16)−C(19)−C(18), 125.7(3); Si(1)−C(18)−C(19), 119.5(2). Selected torsion angles (deg): S(1)−C(4)−C(5)−S(2), −150.59(19); S(2)−C(8)−C(11)−C(10), 16.7(4); C(17)−C(22)−C(23)−S(3), −168.9(2); S(3)−C(26)−C(27)−S(4), 171.58(16).

chromophore by incorporation of a 2,4,6-tris[bis(trimethylsilyl)methyl]phenyl (Tbt) group to prepare silabenzene and higher silaacenes.[30−38] Another rarely studied organosilicon framework is the seven-membered-ring systems, silepins (**III**).[39−56] From a photophysical standpoint they are potentially interesting compounds due to the possibility of aromaticity through Si(3dπ)−C(2pπ) conjugation, although UV−vis[55] and mass spectral analysis[39] do not indicate that this type of electronic communication is significant in published examples. However, red-shifts in absorption[39,40,55] and fluorescence compared to the all-carbon congener, suberene, were seen and are attributed to contribution from the Si−Me σ bonds to the cycloheptatriene π system.[55]

Recently, we reported the use of a seven-membered borepin core in the blue-emitting boron-containing acene analogues, exemplified by dibenzo[*b*,*f*]borepin **IV**.[57] In order to tune the HOMO−LUMO gap of these intriguing materials, we sought to functionalize the periphery of the dibenzoborepin core in the positions *meta* and *para* to boron, as indicated in Chart 1. We thus became interested in the corresponding dibenzo[*b*,*f*]silepins as potential precursors, reasoning that the carbon−silicon bonds of the silepin framework would better withstand the conditions necessary to forge C−C bonds via cross-coupling protocols than the stannepin precursors we utilized in our initial study.[57] In the meantime, Tovar and co-workers reported that suitably

dx.doi.org/10.1021/om2000597 |*Organometallics* 2011, 30, 1719–1729

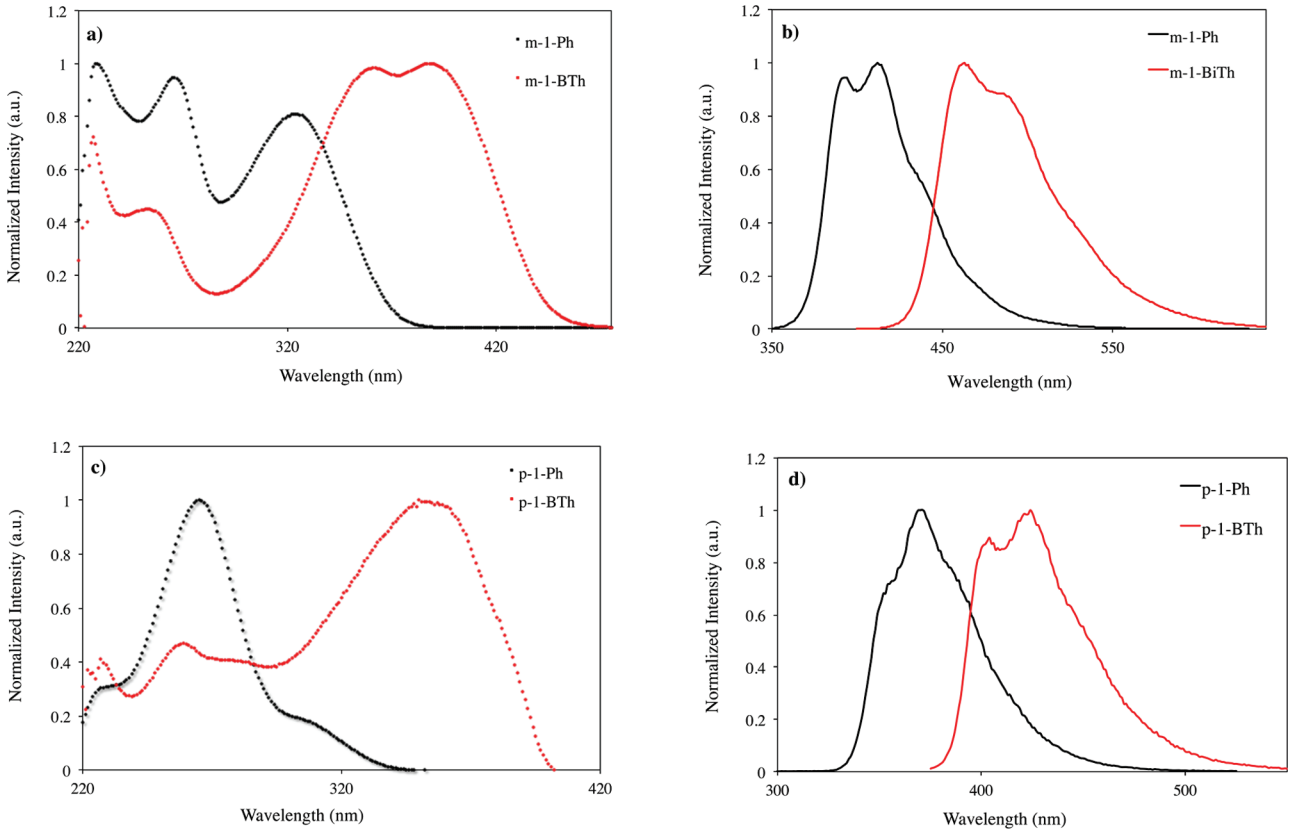

Figure 2. Representative absorption/emission spectra measured in CH_2Cl_2 (5×10^{-5} M): (a) absorbance and (b) fluorescence spectra of ***m*-1-Ph** and ***m*-1-bTh**; (c) absorbance and (d) fluorescence of ***p*-1-Ph** and ***p*-1-bTh**.

sterically shielded borepins themselves could serve as substrates for cross-coupling functionalization reactions without breaching the integrity of the seven-membered core of the molecule and reported their conversion to a number of functionalized borepin targets.[58,59] We show here that conversion of a silepin framework to a borepin function is possible in some instances, but is not generally successful; however, with several *meta*- and *para*-substituted derivatives of **III** in hand, a comparative study between these silepin-based materials and their borepin analogues became possible. Herein we describe the synthesis of a number of novel donor−acceptor−donor (D−A−D) dibenzo[*b*,*f*]silepin-based organic materials that exhibit bathochromic shifts compared to both suberene and the parent, unsubstituted 1,1-dimethyldibenzo[*b*,*f*]silepin (**III**). Comprehensive photophysical and electrochemical measurements, and supporting computational studies, show that for dibenzo[*b*,*f*]silepins with various donor groups in the position *meta* to silicon, silicon acts to rigidify the stilbene framework, while substitution in the *para* position puts the donor groups in direct conjugation with the silicon atom, giving rise to charge-transfer character in their absorption spectra.

RESULTS AND DISCUSSION

Synthesis. The synthetic chemistry relevant to the preparation of the dibenzo[*b*,*f*]silepins is shown in Scheme 1. Synthetic routes to necessary halogenated dibenzo[*b*,*f*]silepins involve both a Wittig reaction between a dihalogen phosphonium aryl salt and a differentiated dihalobenzaldehyde, in keeping with the synthetic strategy we developed for the preparation of dibenzoborepin[57] and also used by Tovar.[58] The chlorobenzaldehydes were synthesized from the corresponding aryl iodide using methodology developed by Knochel,[60] while the phosphonium salts were derived from benzyl bromide derivatives formed via NBS bromination of a dihalotoluene precursor (Scheme S1). Bromobenzaldehydes and bromo-substituted phosphonium salts were prepared from the corresponding commercially available carboxylic acids (Scheme S2). The Wittig reactions afforded the tetrahalo precursors to the *meta* and *para* silepins in excellent yields of 95% and 88% as shown in Scheme 1. The differential halogen substitution was necessary to ensure selective dilithium halogen exchange using *n*BuLi in ether, allowing the aryl dilithium species generated *in situ* to be trapped with dimethyl silicon dichloride to give the compounds ***m*-Cl** (56%) and ***p*-Br** (88%) in workable yields. The addition of TMEDA[58] reduces the presence of polymeric byproduct and facilitates purification.

With these precursors in hand, various C−C coupling protocols were exploited to install a variety of aryl substituents onto the dibenzo[*b*,*f*]silepin core (Table 1). Suzuki coupling reactions were carried out with standard conditions[61] to give fair yields for strongly donating (***m*/*p*-1-PhOMe**, ***m*/*p*-1-PhNPh$_2$**) and moderately donating (***m*/*p*-1-Ph**) aryl groups. Stille coupling conditions[62] were used to prepare thiophene and bithiophene derivatives (***m*/*p*-1-Th**, ***m*/*p*-1-bTh**), while Sonogashira procedures[63] gave the two phenylacetylene-substituted compounds (***m*/*p*-1-CCPh**). The parent, unsubstituted dibenzo[*b*,*f*]silepin

dx.doi.org/10.1021/om2000597 |*Organometallics* 2011, 30, 1719–1729

Table 2. Photophysical and Electrochemical Data for *meta*- and *para*-Substituted Dibenzo[*b*,*f*]silepins[a,b]

compound	abs λ_{onset} [nm]	abs λ_{max} [nm] (log(ε))	fluor λ_{max} [nm]	ϕ_F	τ_f [ns]	$k_{nr}(1-\phi_F)/\tau_f$ [10^8 ns]	$E_{1/2}$ [V]
suberene	332	287(4.22)	384				
		229(4.41)					
1	336	293(4.08)	359	0.14	0.15	57.3	
		243(3.89)	(373)				
			(339)				
***m*-1-Ph**	379	326(3.59)	413	0.90	1.6	0.63	−2.10
		267(3.72)	394				
		229(3.75)					
***m*-1-PhOMe**	385	333(3.71),	424	0.93	1.4	0.50	−2.09
		282(3.67)	(407)				
***m*-1-PhNPh$_2$**	435	357(4.40)	473	0.91	2.1	0.43	−2.22
		305(4.31)					−2.00
		229(4.40)					+1.08 (2e$^-$)
***m*-1-Th**	408	349(3.37)	415	0.77	1.4	1.6	−2.19
		300(3.31)	(438)				−1.93
***m*-1-bTh**	458	389(3.89)	463	0.46	0.94	5.7	−1.92
		361(3.89)	(488)				−1.80
		253(3.55)					
***m*-1-CCPh**	403	347(3.65)	407	0.77	1.2	1.9	−2.01
		299(3.69)	(429)				−1.81
		265(3.51)					
***p*-1-Ph**	338	305(3.74)	371	0.38	1.4	4.4	−2.16
		265(4.47)	(355)				
***p*-1-PhOMe**	334	278(3.78)	391	0.22	5.4	1.4	−2.23
		227(3.26)					
***p*-1-PhNPh$_2$**	390	339(3.82)	447	0.43	5.9	0.97	−2.18
		308(3.78)					+0.96[c]
		253(3.74)					
		228(3.68)					
***p*-1-Th**	354	292(3.95)	394	0.09	2.0	4.6	−2.23
		228(3.57)					
***p*-1-bTh**	398	350(3.42)	424	0.10	0.47	19.1	−2.24
		259(3.09)	(404)				
		227(3.03)					
***p*-1-CCPh**	346	310(3.74)	375	0.36	3.8	1.7	−2.03
		291(3.80)					
		226(3.47)					

[a] Absorption and fluorescence were measured in 5×10^{-5} M DCM solution. [b] Cyclic voltammetry was carried out at a scan rate of 100 mV/s in THF with 1 mM substrate and 0.1 M [NBu_4][PF_6] as the supporting electrolyte. Ferrocene (Fc/Fc^+) was used as an internal standard and set to 0.54 V. [c] Cyclic voltammetry was carried out at a scan rate of 100 mV/s in DCM with 1 mM substrate and 0.1 M [NBu_4][PF_6] as the supporting electrolyte. Ferrocene (Fc/Fc^+) was used as an internal standard and set to 0.47 V.

was prepared for comparison by a similar procedure, using a dibromostilbene precursor as shown in eq 1.

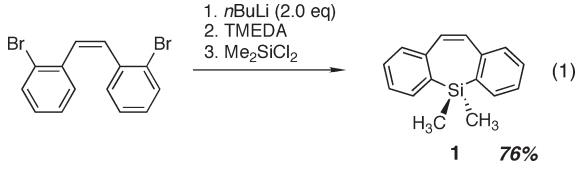

(1)

1 **76%**

All of the π-extended silepins reported here are air and moisture stable and were purified by column chromatography. They were fully characterized using NMR spectroscopy and high-resolution mass spectrometry. In the ^{29}Si NMR, the chemical shift of the silepin silicon was not strongly affected by the substitution differences. Unsubstituted **1** was observed at −10.9 ppm relative to $SiMe_4$; the *meta* derivatives were slightly downfield of this value (−10.2 to −10.4 ppm), while the *para* series appeared marginally upfield (−10.6 to −11.4 ppm). In common organic solvents (hexanes, toluene, methylene chloride) the compounds give pale yellow or colorless solutions. Photostability studies in solution indicate that they slowly, but not completely, decompose when exposed in a light box to 254 nm light for >12 h. Drop cast solid films of ***p*-1-PhOMe** demonstrated even less photodegradation (<3−4%) when irradiated for 24 h at 254 nm. The primary products from these photoreactions appear to be formed via photoejection of "$SiMe_2$", based on the mass spectrometric

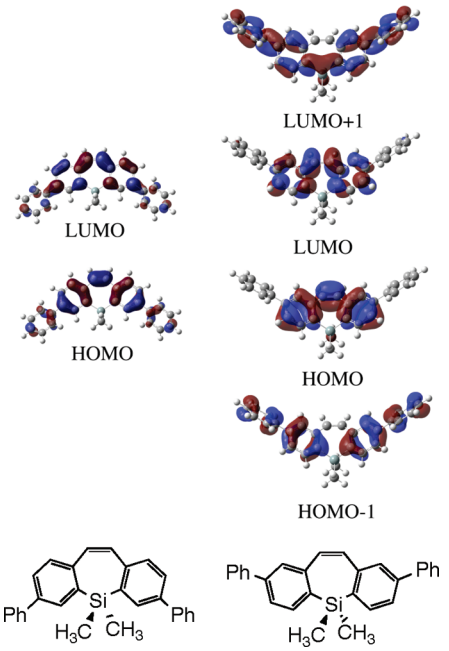

Figure 3. Representative HOMO and LUMO orbital surfaces for ***m*-1-Ph** (left) and ***p*-1-Ph** (right) calculated at the B3LYP/6-31G(d,p) level using Gaussian 03.

detection of substituted phenanthrenes. However, these reactions are not clean, and rigorous determination of the photodecomposition pathways has not been done.

Despite the fact that all of these silepins are solids under ambient conditions, X-ray quality crystals were difficult to come by; the crystal habit of the compounds tends toward long needles that do not strongly diffract. The connectivity in compound ***p*-1-Ph** was established positively, but the *R*-factor of ∼30% results in metrical data with a low level of precision (see Figure S1). However, one exception was the compound ***m*-1-bTh**, whose structure was successfully determined; its molecular structure is shown in Figure 1, along with selected metrical parameters. The molecule assumes an overall bent shape due to the boat-like conformation of the central silepin ring, where C(15)−C(16) forms the stern and the Si(1)Me_2 unit the prow. As a result, the angle between the planes defined by the C_6 rings flanking the silepin core is 123.18(9)°. The bond distance of 1.343(4) Å for C(15)−C(16) is typical for a C=C bond, but due to the strain found in the seven-membered ring, the C(14)−C(15)−C(16) and C(15)−C(16)−C(19) angles are 10−12° greater than the ideal value of 120°. Ring strain also results in longer bonds from C(9) and C(18) to Si(1) than those to the sp^3-hybridized carbons C(31) and C(32). The bithiophene units exhibit good conjugation with the aromatic rings of the dibenzosilepin, as judged by torsion angles about C(8)−C(11) and C(22)−C(23) that are less than 17° away from coplanarity. The bithiophene torsion angles about C(4)−C(5) and C(26)−C(27) are somewhat different, with the former being about 30° from coplanarity in contrast to the latter, which has an S(3)−C(26)−C(27)−S(4) dihedral angle of 171.58(16)°.

Photophysical and Electrochemical Data. The absorption and emission spectra for ***m*/*p*-1-Ph** and ***m*/*p*-1-bTh** are shown in Figure 2 as typical examples of these two families of compounds; a complete summary of the photophysical and electrochemical data obtained is given in Table 2.[64] Within the *meta* series of compounds, it is apparent that as donating group strength and conjugation length increase, there is a bathochromic shift in both the longest absorption and fluorescence maxima compared to unsubstituted **1** (Table 2). Compound ***m*-1-Ph** displays the weakest red-shift in both onset absorption (43 nm) and emission maxima (54 nm), while introduction of more extensively conjugated groups as in ***m*-1-PhOMe** and ***m*-1-PhNPh$_2$** shows larger shifts in absorption (up to 56 nm) and emission (up to 80 nm). The phenylacetylene (***m*-1-CCPh**) and thiophene (***m*-1-Th**) derivatives display moderate changes, while an increase in donor strength and conjugation length in ***m*-1-bTh** gives a very large red-shift of 122 nm in onset absorption and of 56 nm in emission maxima. Solvatochromism studies (Table S1) show small positive effects when a strongly donating group is present, for example in ***m*-1-NPh$_2$**. In this instance, the HOMO surface is mainly associated with the donor group, while the LUMO is largely located on the dibenzo[*b*,*f*]silepin core, resulting in a degree of charge separation in the excited state. Other members of the *meta* family exhibit little solvatochromism, since the HOMOs and LUMOs are more diffusely conjugated over the entire framework, resulting in little change in the dipole moments of ground versus excited states. All of the *meta* series compounds show high fluorescence quantum yields and short fluorescence lifetimes, which indicates short nonradiative decay rate constants.

In the *para* series of substituted silepins, the donating substituents are introduced in a position that puts them in conjugation with the silicon atom and not only extends the π framework but also increases charge-transfer character from the donating groups to the silepin ring. Solvatochromism patterns in this series (Table S1) show large red-shifts in polar solvents for silepins substituted with strongly donating groups, which indicates significant charge transfer in the excited state. This is supported by a Lippert−Mataga plot[65−67] (Figure S3), which revealed large changes in dipole moment between ground and excited states for ***p*-1-PhNPh$_2$** and ***p*-1-PhOMe** (35.0 and 18.4 D, respectively). In the *meta*-substituted family, smaller differences were seen for ***m*-1-PhNPh$_2$** and ***m*-1-bTh** (23.8 and 14.2 D). Compared to the *meta*-substituted compounds, smaller bathochromic shifts in onset absorption and emission maxima are seen for the *para* series. For example, compound ***p*-1-Ph** exhibits similar onset absorptions and emission maxima to **1**; this is probably due to the orthogonality of the phenyl rings, as indicated by the computed structure for this derivative (see below). Introduction of an electron-donating group to the phenyl ring, as seen for ***p*-1-PhOMe** and ***p*-1-PhNPh$_2$**, shows large shifts in emission maxima relative to **1** (32 and 54 nm, respectively), suggesting a higher level of electronic communication from these aryl groups to the silepin core. Compounds ***p*-1-Th** and ***p*-1-bTh** show strong red-shifts in both onset absorption (18 nm, 62 nm) and fluorescence (35, 65 nm) profiles. The *para* series shows moderate quantum yields, lower than those seen in the *meta* series, and longer fluorescence lifetime; therefore the rates of nonradiative decay processes are larger.

Computations. The absorption behavior of these compounds as described above would seem to suggest that the *meta* series essentially functions as a rigidified stilbene chromophore in which the dimethylsilyl group serves as an anchoring group with little ability to perturb the HOMO−LUMO character of the molecule. In contrast, in the *para* series absorptions with more charge-transfer character begin to compete with the $\pi-\pi^*$ transitions that dominate the *meta* compounds. This notion is supported by TD-DFT calculations using Gaussian 03, which for

Table 3. Molecular Orbital Energies, Energy Gaps, and Oscillator Strengths Taken from Calculations Run at the B3LYP/6-31G(d,p) Level[a]

Compound	HOMO−1 [eV]	HOMO [eV]	LUMO [eV]	LUMO+1 [eV]	transition energy[b] [eV]	oscillator strength[b] (*f*)
***m*-1-Ph**	−6.27	−5.32	−1.65	−0.56	3.31	0.9338
***m*-1-PhOMe**	−5.89	−5.40	−1.56	−0.69	3.42	0.9042
***m*-1-PhNPh$_2$**	−4.97	−4.81	−1.60	−0.65	2.83	1.1773
***m*-1-Th**	−6.12	−5.58	−1.92	−1.15	3.28	0.8417
***m*-1-bTh**	−5.69	−4.99	−2.17	−1.65	2.70	1.2913
***m*-1-CCPh**	−6.10	−5.66	−2.21	−1.45	3.08	1.2555
***p*-1-Ph**	−6.28	−5.95	−1.56	−1.18	3.98 (4.64)[c]	0.3505 (1.4586)[c]
***p*-1-PhOMe**	−5.79	−5.76	−1.44	−0.973	3.83 (4.38)[c]	0.0221 (0.9645)[c]
***p*-1-PhNPh$_2$**	−5.19	−5.18	−1.53	−1.21	3.29 (3.52)[c]	0.0633 (1.0863)[c]
***p*-1-Th**	−6.08	−5.81	−1.88	−1.43	3.55 (4.21)[c]	0.1067 (1.3879)[c]
***p*-1-bTh**	−5.61	−5.56	−1.82	−1.81	3.56	1.2030
***p*-1-CCPh**	−6.05	−6.03	−1.88	−1.72	3.68 (3.85)[c]	0.0030 (1.6983)[c]

[a] Frontier molecular orbital energies from optimized DFT calculations. [b] Oscillator strengths and energy of transitions from TD-DFT calculations. [c] Oscillator strengths and energy of transitions from filled orbitals to the LUMO+1 orbital.

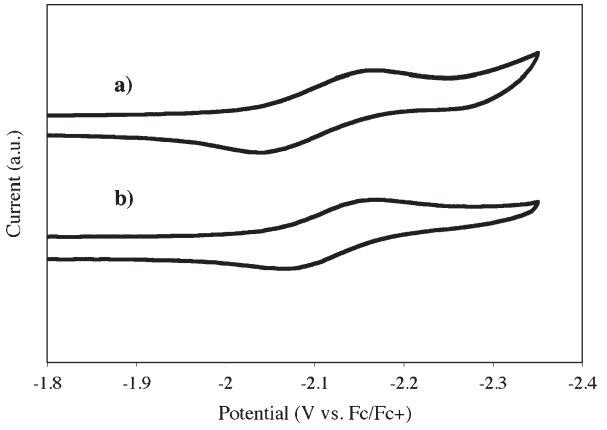

Figure 4. Representative cyclic voltammetry (CV) curves for (a) ***m*-1-Ph** and (b) ***p*-1-Ph** measured at 100 mV/s in THF with 1 mM substrate and 0.1 M [NBu_4][PF_6] as the supporting electrolyte. Ferrocene (Fc/Fc^+) was used as an internal standard and set to 0.54 V.

the *meta* series show strong oscillator strengths for HOMO to LUMO absorptions that correspond to $\pi-\pi^*$ transitions based on the fully conjugated stilbene framework (Figure S4). This is exemplified by the HOMO/LUMO orbitals for ***m*-1-Ph** shown in Figure 3 and the computed HOMO/LUMO energies and oscillator strength data given in Table 3. For the corresponding ***p*-1-Ph** isomer, the HOMO/LUMO combination is again suggestive of a $\pi-\pi^*$ transition, but in these compounds, the LUMO+1 orbital is very close in energy to the LUMO and has strong C−Si−C σ^* character, showing silicon does more than simply rigidify the stilbene and acts as an acceptor group (Figure 3, Figure S5). Indeed, the TD-DFT analysis shows that these HOMO to LUMO+1 transitions have high oscillator strengths (Table 3).

Electrochemistry. Cyclic voltammetry was carried out on all the silepins reported here to obtain a measurement of the HOMO/LUMO gap. All compounds exhibited reversible one-electron reduction waves; for several members of the *meta* series, a second reduction was also observed (Figure 4, Figure S6). Overall, the *meta* compounds were more easily reduced than the *para* compounds, meaning their LUMO orbitals were more stabilized. Ionization potentials (HOMO) and electron affinities

Table 4. Frontier Orbital Energies Derived from Electrochemical Data and UV−Vis Onset Absorptions for *meta*- and *para*-Substituted Silepins

compound	LUMO[a] [eV]	HOMO[b] [eV]	E_g[c] [eV]
***m*-1-Ph**	−2.1	−5.4	3.3
***m*-1-PhOMe**	−2.1	−5.3	3.2
***m*-1-PhNPh$_2$**	−2.2	−5.0	2.9
***m*-1-Th**	−2.3	−5.3	3.0
***m*-1-bTh**	−2.4	−5.1	2.7
***m*-1-CCPh**	−2.4	−5.5	3.1
***p*-1-Ph**	−2.0	−5.7	3.6
***p*-1-PhOMe**	−1.9	−5.6	4.1
***p*-1-PhNPh$_2$**	−2.1	−5.3	3.2
***p*-1-Th**	−1.8	−5.3	3.5
***p*-1-bTh**	−2.1	−5.2	3.1
***p*-1-CCPh**	−2.1	−5.7	3.6

[a] Calculated from E_{pc} of first reduction wave referenced to Fc/Fc^+ ($E_{1/2}$ = −4.8 eV). [b] Calculated from $E_{1/2}$ and onset absorption energy. [c] Onset absorption energy.

(LUMO) were derived from E_{pc} (Fc/Fc^+ $E_{1/2}$ = −4.80 eV)[68] and onset absorption (Table 4). For the *meta*-substituted silepins, the energy of the HOMO increases with conjugation length and LUMO energy is lowered as the groups interact favorably with the silepin core, for example in ***m*-1-bTh** and ***m*-1-CCPh**. In the *para* series, compounds ***p*-1-BTh** and ***p*-1-CCPh** have the most stabilized LUMO levels due to the extended conjugation framework in these derivatives. The HOMO energies see similar modifications to those in the *meta* series, and red-shifts observed are mainly derived from conjugation length. The HOMO/LUMO gap resulting from these measurements are in excellent agreement with those obtained from the TD-DFT computations (see Table 3).

Comparison with Substituted Borepins. In a closely related study,[59] Tovar and Caruso report a series of *meta*- and *para*-substituted dibenzoborepins with a similar array of substituents to those reported here for the silepins **1**, and a comparison of the behavior of the two families of compounds is instructive. In general, the directly comparable systems (those with *meta* and *para* PhOMe, Th, bTh, and CCPh substituents) show that the

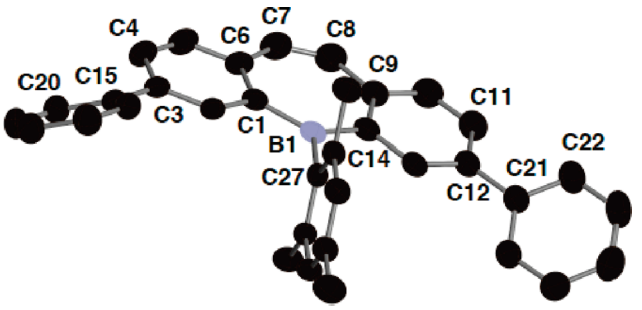

Figure 5. Displacement ellipsoid diagram (50% probability level) for the molecular structure of ***m*-2-Ph**. Selected bond distances (Å): B(1)−C(1), 1.564(3); B(1)−C(14), 1.564(3); B(1)−C(27), 1.588(3); C(1)−C(6), 1.427(3); C(6)−C(7), 1.438(3); C(7)−C(8), 1.345(3); C(8)−C(9), 1.442(3); C(9)−C(14), 1.427(3). Selected bond angles (deg): C(1)−B(1)−C(14), 127.42(17); C(6)−C(7)−C(8), 133.1(2); C(7)−C(8)−C(9), 133.8(2). Selected torsion angles (deg): C(4)−C(3)−C(15)−C(20), −35.4(3); C(11)−C(12)−C(21)−C(22), −36.1(3).

onset absorptions for the silepins are at higher energy, indicating a larger HOMO/LUMO gap in the silicon compounds. This can be attributed to the boron-centered LUMO in the Lewis acidic borepins. In both families of compounds, substitutions result in red-shifts when compared to the parent, unsubstituted silepin (**1**), and both families exhibit larger red-shifts for the *meta* series than the *para* derivatives. In general, the silepins exhibit greater quantum yields (the values in Table 1 are absolute quantum yields) and larger Stokes shifts than the borepins. The larger Stokes shifts in the silepins may be rooted in bent-to-planar geometry changes[69] from ground-state structures to excited states; in the planar borepins, these changes are likely to be less significant. However, the photophysical properties between these families of chromophores are not phenomonologically very different, but because in the planar borepins the empty p orbital on boron is conjugated with the rest of the π system, the character of the HOMO/LUMO absorptions in the boron heterocycles have less charge-transfer character. In the silepins, the chromophores are more similar to rigidified stilbenes, and charge-transfer character emerges only when strongly donating substituents are incorporated and HOMO → LUMO+1 transitions dominate.

Conversion of Silepins to Borepins. Synthetic routes to both families proceed through differentially halogenated tetrahalostilbenes, with the borepins requiring an extra transmetalation step from the precusor stannepins. In fact, the silepins can also be used as precurors to borepins; as shown in eq 2, ***m*-1-Ph** can be converted to the B-mesityl borepin ***m*-2-Ph** after quenching the *in situ*-generated borepin bromide with mesityllithium. X-ray quality crystals of this material were obtained after purification by column

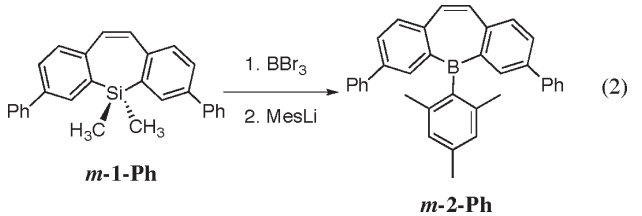

***m*-1-Ph** ***m*-2-Ph** (2)

chromatography, and a displacement ellipsoid diagram is given in Figure 5, along with selected metrical parameters. In contrast to the parent, unsubstituted dibenzoborepin, which exhibited substantial curvature in the tricyclic ring system,[57] the borepin core in ***m*-2-Ph** is completely planar, in keeping with computational prediction. Here, incorporation of the *meta* phenyl groups disrupts the packing interactions that result in the previously observed curvature. The bond distances within ***m*-2-Ph** are as expected, and the internal ring angles for the seven-membered ring exhibit similar patterns to those described above for ***m*-1-bTh**. The torsion angles given show that the two phenyl groups are twisted out of coplanarity with the dibenzoborepin core to an extent typical of biphenyl compounds.

Although this particular silepin to borepin conversion was successful, when NPh_2 groups were present, side reactions between BBr_3 and the Lewis basic groups precluded conversion to the borepins via this route. The other derivatives would likely suffer from this issue also; thus, the Tovar strategy of carrying out coupling reactions directly on the dihaloborepin precursors appears to be more general than a pathway that sequences the coupling reactions before the transmetalation step.

CONCLUSIONS

A family of *meta*- and *para*-substituted silepins were prepared via standard aryl coupling reactions and exhibited red-shifted absorption and emission compared to the parent 1,1-dimethyldibenzo[b,f]silepin (**1**). In the *meta* position, these changes have been attributed to an increase in overall conjugation of the stilbene framework where silicon rigidifies the system, raising the energy of the HOMO level. The degree of bathochromic shifting is dependent on the nature of the donor group, which lowers the LUMO level as it becomes more energetically compatible with silepin core. When electron donor groups are coupled in the *para* position, smaller bathochromic shifts in onset absorption and fluorescence are observed since the HOMO−LUMO gap is mostly affected by the raising of HOMO energy. For strongly donating groups (e.g., in ***m*-1-NPh$_2$**), strong positive solvatochromism is observed in the *para* case, suggesting charge-transfer character in some of these systems; computations indicate this involves excitation into the LUMO+1 levels, which have a strong contribution from the σ^* orbitals of the core C−Si−C bonds. The *para* series also show larger nonradiative decay processes since they have lower quantum yields and longer fluorescence lifetimes than the *meta* series and are less easily reduced. Overall, these compounds exhibit strong blue fluorescence and are air and moisture stable—excellent candidates for applications as organic materials.

EXPERIMENTAL SECTION

General Procedures and Equipment. All reactions and product manipulations were performed under a purified argon atmosphere using vacuum line techniques or in an MBraun glovebox unless otherwise specified. All solvents were dried over the appropriate drying agents (activated alumina, CaH_2, Na/benzophenone) and vacuum distilled prior to use. Silica gel column chromatography was carried out on Silia-P Flash silica gel (particle size 40−63 mm) from Silicycle. Potassium *tert*-butoxide, *n*BuLi (1.6 M in hexanes), and 4-bromo-2-iodobenzoic acid (Trans World Chemicals Inc.) were used as received. Triphenylphosphine, dichlorodimethylsilane, 1-bromo-4-chlorobenzene, dimethylformamide, 4-chloroaniline, and 4-chlorotoluene were used as received from Aldrich. Dimethylformamide was dried with magnesium sulfate, distilled under reduced pressure, and stored over molecular sieves. These materials were employed to prepare the tetrahalogenated precursors to the silepins ***m*/*p*-1-Ar** as depicted in Schemes S1 and S2; a

dx.doi.org/10.1021/om2000597 |*Organometallics* 2011, 30, 1719–1729

description of the synthesis of unknown materials is also given in the SI. All NMR spectra were recorded from solutions in dry, oxygen-free $CDCl_3$ on a Bruker UGI-400 MHz, Bruker RDQ-400 MHz, or Bruker DRY-400 MHz spectrometer operating at 400 MHz (^{1}H), 79 MHz (^{29}Si), or 100 MHz (^{13}C) at 25 °C unless otherwise specified. Chemical shifts are reported relative to $SiMe_4$ (^{29}Si) or to $CDCl_3$ calibrated to 7.26 ppm (^{1}H) and 77.0 ppm (^{13}C). Where required, ^{1}H and ^{13}C peak assignments were made using ^{1}H−^{1}H COSY or ^{1}H−^{13}C HMQC 2D spectra. High-resolution mass spectra were obtained on a Kratos MS-80 spectrometer operating in electron impact (EI) mode, HR-MALDI spectra were recorded on a Bruker Autoflex III MALDI-Tof/Tof with Smartbeam laser system, and HR-APCI were obtained on a Bruker Escquire 3000 with ESI, APCI, and nanospray sources, LC (Agilent 1100 with autosampler), and direct syringe infusion. Fluorescence spectra were obtained on a Horiba Jobin Yvon FluoroMax-4, and UV−visible spectra were obtained on a Varian Cary 5000 UV−vis−NIR spectrophotometer operating in single-beam mode. Absolute fluorescence quantum yield values were measured using an Edinburgh Instruments FLS92 calibrated integrating sphere system. Fluorescence lifetime experiments were performed on the Edinburgh Instruments FLS920 using a reconvolution fit. High-resolution mass spectra were obtained on a Kratos MS-80 spectrometer operating in electron impact (EI) mode. X-ray crystallographic analyses were performed on suitable crystals coated in Paratone oil and mounted on Oxford Diffraction Gemini A Ultra and Nonius KappaCCD diffractometers. Computations were performed using the Gaussian 03 suite of programs.[70]

Synthesis of ***1***. The procedure below is modified from a recent literature report.[58] *n*BuLi (1.6 M in hexanes, 0.59 mL) was added to a solution of (*Z*)-1,2-bis(2-bromophenyl)ethene (159 mg, 0.47 mmol) in diethyl ether (23 mL) at −78 °C, and the solution turned yellow. After 30 min, tetramethylethanediamine (0.15 mL, 1.03 mmol) was added, and the solution was stirred for 2 h at −78 °C. Neat dimethylsilicon dichloride (0.06 mL, 0.52 mmol) was added dropwise, and the solution eventually turned yellow. It was allowed to gradually warm to room temperature over 16 h, at which time the reaction was quenched with a mixture of water and ether (1:1) and the aqueous layer extracted with ether. Combined organic extracts were washed with hydrochloric acid (0.2 N), water, and brine, dried with anhydrous $MgSO_4$, filtered, and the solvent was removed *in vacuo*. The crude product was purified by column chromatography (SiO_2, hexanes) to yield **1** (84.3 mg, 76%) as a yellow oil. ^{1}H NMR ($CDCl_3$): δ 7.60 (ddd, J_{HH} = 7.2 Hz, 1.2 Hz, 1.2 Hz 2H), 7.40−7.35 (m, 6H), 7.00 (s, 2H), 0.52 (s, J_{Si-H} = 120.1 Hz, 6H) ppm. ^{13}C{^{1}H} NMR ($CDCl_3$): δ 141.4, 137.2, 133.1, 132.5, 129.4, 128.9, 127.3, −4.7 ppm. ^{29}Si{^{1}H} NMR ($CDCl_3$): δ −10.9 ppm. HRMS: calcd for $C_{16}H_{16}Si$ [M^+] 236.1021, found 236.1025.

Synthesis of ***m-1-Cl***. *n*BuLi (1.6 M in hexanes, 8.4 mL) was added to a solution of (*Z*)-1,2-bis(2-bromo-4-chlorophenyl)ethene (2.6 g, 6.4 mmol) in diethyl ether (320 mL) at −78 °C, and the solution turned orange then brown in color. After 30 min, tetramethylethanediamine (2.1 mL, 14.1 mmol) was added, and the solution was stirred for 2 h at −78 °C. Neat dimethylsilicon dichloride (0.85 mL, 7.04 mmol) was added dropwise, and the solution eventually turned yellow. It was allowed to gradually warm to room temperature over 16 h, at which time the reaction was quenched with a mixture of water and ether (1:1) and the aqueous layer extracted with ether. Combined organic extracts were washed with hydrochloric acid (0.2 N), water, and brine, dried with anhydrous $MgSO_4$, filtered, and the solvent was removed *in vacuo*. The crude product was purified by column chromatography (SiO_2, hexanes) to yield ***m*-1-Cl** (1.10 g, 56%) as an off-white solid. ^{1}H NMR ($CDCl_3$): δ 7.48 (d, J_{HH} = 2.0 Hz, 2H), 7.33 (dd, J_{HH} = 8.4 Hz, 2.0 Hz, 2H), 7.29 (d, J_{HH} = 8.4 Hz, 2H), 6.92 (s, 2H), 0.50 (s, 6H) ppm. ^{13}C{^{1}H} NMR ($CDCl_3$): δ 139.4, 138.8, 134.2, 132.3, 132.2, 131.0, 129.1, −5.0 ppm. ^{29}Si{^{1}H} NMR ($CDCl_3$): δ −10.2 ppm. HRMS (EI): calcd for $C_{16}H_{14}SiCl_2$ [M^+] 304.0242, found 304.0249.

Synthesis of ***p-1-Br***. *n*BuLi (1.6 M in hexanes, 1.1 mL) was added to a solution of (*Z*)-1,2-bis(5-bromo-2-iodophenyl)ethene (0.50 g, 0.85 mmol) in diethyl ether (43 mL) at −78 °C, and the solution turned orange-red in color. After 30 min, tetramethylethanediamine (0.28 mL, 1.87 mmol) was added, and the solution was stirred for 2 h at −78 °C. Neat dimethylsilicon dichloride (0.11 mL, 0.94 mmol) was added dropwise, and the solution eventually turned yellow. It was allowed to gradually warm to room temperature over 16 h, at which time the reaction was quenched with a mixture of water and ether (1:1) and the aqueous layer extracted with ether. Combined organic extracts were washed with hydrochloric acid (0.2 N), water, and brine, dried with anhydrous $MgSO_4$, filtered, and the solvent removed *in vacuo*. The crude product was purified by column chromatography (SiO_2, hexanes) to yield ***p*-1-Br** (0.23 g, 68%) as a yellow gum-like substance. ^{1}H NMR ($CDCl_3$): δ 7.52 (d, J_{HH} = 1.8 Hz, 2H), 7.47 (dd, J_{HH} = 7.9 Hz, 1.8 Hz, 2H), 7.40 (d, J_{HH} = 7.9 Hz, 2H), 6.90 (s, 2H), 0.48 (s, 6H) ppm. ^{13}C{^{1}H} NMR ($CDCl_3$): δ 142.8, 135.7, 134.0, 132.8, 132.1, 130.5, 123.7, −4.8 ppm. ^{29}Si{^{1}H} NMR ($CDCl_3$): δ −10.2 ppm. HRMS (EI): calcd for $C_{16}H_{14}SiBr_2$ [M^+] 393.9211, found 393.9204.

General Procedure for Suzuki Coupling Reactions. The Suzuki couplings were accomplished using a procedure based on that reported by Buchwald and co-workers.[61] A clean dried flask was charged with ***m*-1-Cl** or ***p*-1-Br** (0.05 mmol), K_3PO_4 (0.20 mmol), boronic acid (0.15 mmol), $Pd(OAc)_2$ (4 mol %), and SPhos (8 mol %). Degassed water (0.1 mL) was added under an atmosphere of argon, and the mixture was stirred for 5 min. Toluene (1 mL) was then added, and the suspension heated to reflux for 16 h. The reaction was cooled to room temperature and filtered over silica, and solvent was removed *in vacuo*. Crude product was purified by column chromatography.

Data for ***m-1-Ph***. The crude product was purified by column chromatography (SiO_2, hexanes −3% EtOAc/hexanes) to yield ***m*-1-Ph** (12.6 mg, 65%) as a white solid. ^{1}H NMR ($CDCl_3$): δ 7.80 (d, J_{HH} = 2.0 Hz, 2H), 7.60 (ddd, J_{HH} = 7.2, 1.3, 1.3 Hz, 6H), 7.48−7.43 (m, 6H), 7.36 (tdd, J_{HH} = 7.3, 1.5, 1.5 Hz, 2H), 7.05 (s, 2H), 0.60 (s, 6H) ppm. ^{13}C{^{1}H} NMR ($CDCl_3$): δ 141.0, 140.5, 140.2, 137.4, 132.8, 131.3, 130.1, 128.8, 127.8, 127.3, 127.2, −4.5 ppm. ^{29}Si NMR ($CDCl_3$): δ −10.3 ppm. HRMS (EI): calcd for $C_{28}H_{24}Si$ [M^+] 388.1647, found 388.1647.

Data for ***p-1-Ph***. The crude product was purified by column chromatography (SiO_2, hexanes −3% EtOAc/hexanes) to yield ***p*-1-Ph** (19.2 mg, 88%) as a white solid. ^{1}H NMR ($CDCl_3$): δ 7.67 (dd, J_{HH} = 7.7, 0.4 Hz, 2H), 7.62 (dd, J_{HH} = 1.7, 0.9 Hz, 2H), 7.61−7.60 (m, 2H), 7.59−7.56 (m, 2H), 7.56 (d, J_{HH} = 1.7 Hz, 2H), 7.44 (dddd, J_{HH} = 7.4, 1.2, 1.2, 0.9 Hz, 4H), 7.34 (tdd, J_{HH} = 6.7, 2.0,1.7 Hz, 2H), 7.10 (s, 2H), 0.58 (s, 6H) ppm. ^{13}C{^{1}H} NMR ($CDCl_3$): δ 141.9, 141.8, 140.9, 136.0, 133.5, 133.1, 128.8, 128.2, 127.4, 127.2, 126.2, −4.5 ppm. ^{29}Si NMR ($CDCl_3$): δ −10.9 ppm. HRMS (EI): calcd for $C_{28}H_{24}Si$ [M^+] 388.1647, found 388.1646.

Data for ***m-1-PhOMe***. The crude product was purified by column chromatography (SiO_2, 10−50% dichloromethane/hexanes) to yield ***m*-1-PhOMe** (15.8 mg, 70%) as a yellow solid. ^{1}H NMR ($CDCl_3$): δ 7.78 (d, J_{HH} = 2.0 Hz, 2H), 7.58−7.54 (m, 6H), 7.45 (d, J_{HH} = 8.0 Hz, 2H), 7.03 (s, 2H), 7.00 (ddd, J_{HH} = 6.7, 2.6, 2.4 Hz, 4H), 3.86 (s, 6H), 0.59 (s, 6H) ppm. ^{13}C{^{1}H} NMR ($CDCl_3$): δ 159.2, 140.0, 139.7, 137.3, 133.6, 132.6, 130.8, 130.1, 128.1, 127.4, 114.2, 55.3, −4.6 ppm. ^{29}Si NMR ($CDCl_3$): δ −10.4 ppm. HRMS (APCI): calcd for $C_{30}H_{28}O_2Si$ [M^+ + H] 449.193133, found 449.193574.

Data for ***p-1-PhOMe***. The crude product was purified by column chromatography (SiO_2, 10% ethyl acetate/hexanes) to yield ***p*-1-PhOMe** (11.1 mg, 95%) as a yellow solid. ^{1}H NMR ($CDCl_3$): δ 7.63 (d, J_{HH} = 7.6 Hz, 2H), 7.57 (s, 2H), 7.53 (d, J_{HH} = 8.0 Hz, 6H), 7.08 (s, 2H), 6.98 (d, J_{HH} = 8.4 Hz, 4H), 3.85 (s, 6H), 0.56 (s, 6H) ppm. ^{13}C{^{1}H} NMR ($CDCl_3$): δ 159.3, 141.8, 141.5, 135.4, 133.5, 133.4, 133.1, 128.1, 127.8, 125.8, 114.2, 55.4, −4.5 ppm. ^{29}Si NMR ($CDCl_3$): δ −11.4 ppm. HRMS (APCI): calcd for $C_{30}H_{28}O_2Si$ [M^++H]; 449.193113, found 449.193289.

Data for ***m-1-PhNPh$_2$***. The crude product was purified by gel permeation chromatography (DCM, 4 mL/min, t_R = 9.23 min) to yield ***m*-1-PhNPh$_2$** (from 0.100 mmol, 46.4 mg, 64%) as a bright yellow solid. ^{1}H NMR ($CDCl_3$): δ 7.78 (d, J_{HH} = 2.0 Hz, 2H), 7.57 (dd, J_{HH} = 8.0 Hz, 2.0 Hz, 2H), 7.49 (d, J_{HH} = 8.4 Hz, 4H), 7.44 (d, J_{HH} = 8.0 Hz, 2H), 7.30−7.25 (m, 8H), 7.15 (d, J_{HH} = 8.0 Hz, 12H), 7.04 (dd, J_{HH} = 7.4 Hz, 7.4 Hz, 4H), 7.01 (s, 2H) 0.59 (s, 6H) ppm. $^{13}C\{^1H\}$ NMR ($CDCl_3$): δ 147.7, 147.3, 140.2, 139.6, 137.3, 134.9, 132.7, 130.8, 130.1, 129.3, 127.8, 127.3, 124.5, 123.9, 123.0, −4.5. ^{29}Si NMR ($CDCl_3$): δ −10.3 ppm. HRMS (APCI): calcd for $C_{52}H_{43}N_2Si$ [M^+ + H]; 723.319002, found 723.316968.

Data for ***p-1-PhNPh$_2$***. The crude product was purified by column chromatography (SiO_2, 10% EtOAc/hex) to yield ***p*-1-PhNPh$_2$** (6.3 mg, 41%) as fine white needles. ^{1}H NMR ($CDCl_3$): δ 7.63 (d, J_{HH} = 7.7 Hz, 2H), 7.58 (d, J_{HH} = 1.4 Hz, 2H), 7.53 (dd, J_{HH} = 7.7 Hz, 1.8 Hz, 2H), 7.46 (ddd, J_{HH} = 8.8 Hz, 2.4 Hz, 2.4 Hz, 4H), 7.29−7.25 (m, 8H), 7.14−7.11 (m, 12H) 7.06 (s, 2H), 7.03 (ddd, J_{HH} = 7.32 Hz, 1.2 Hz, 1.2 Hz, 4H), 0.55 (s, 6H) ppm. $^{13}C\{^1H\}$ NMR ($CDCl_3$): δ 147.6, 147.4, 141.8, 141.4, 135.5, 134.7, 133.5, 133.1, 129.3, 127.82, 127.8, 125.7, 124.5, 123.7, 123.0, −4.5. ^{29}Si NMR ($CDCl_3$): δ −11.4 ppm. HRMS (APCI): calcd for $C_{52}H_{43}N_2Si$ [M^+ + H] 723.319002, found 722.319744.

General Procedure for Stille Coupling Reactions. The Stille couplings were accomplished using a procedure based on that reported by Fu and co-workers.[62] A clean dried flask was charged with ***m*-1-Cl** or ***p*-1-Br** (0.05 mmol), CsF (0.22 mmol), stannane (0.13 mmol), Pd-$(PPh_3)_4$ (5 mol %), and P*t*Bu$_3$ (10 mol %). Dioxane (1 mL) was added and the suspension heated to reflux for 36 h. The reaction was cooled to room temperature and filtered over silica, and solvent was removed *in vacuo*. The crude product was purified by column chromatography.

Data for ***m-1-Th***. The crude product was purified by column chromatography (SiO_2, 5−20% DCM/hexanes) to yield ***m*-1-Th** (13.2 mg, 66%) as a yellow solid. ^{1}H NMR ($CDCl_3$): δ 7.80 (d, J_{HH} = 2.0 Hz, 2H), 7.61 (dd, J_{HH} = 8.0 Hz, 2.0 Hz, 2H), 7.39 (d, J_{HH} = 8.0 Hz, 2H), 7.33 (dd, J_{HH} = 3.6 Hz, 1.1 Hz, 2H), 7.29 (dd, J_{HH} = 5.1 Hz, 1.1 Hz, 2H), 7.09 (dd, J_{HH} = 5.1 Hz, 3.6 Hz, 2H), 6.97 (s, 2H), 0.59 (s, 6H) ppm; $^{13}C\{^1H\}$ NMR ($CDCl_3$): δ 144.3, 140.7, 137.4, 133.4, 132.7, 130.2, 130.0, 128.1, 126.6, 125.0, 123.2, −4.7 ppm. ^{29}Si NMR ($CDCl_3$): δ −10.3 ppm. HRMS (EI): calcd for $C_{24}H_{20}S_2Si$ [M^+] 400.0776, found 400.0793.

Data for ***p-1-Th***. The crude product was purified by column chromatography (SiO_2, 5−20% DCM/hexanes) to yield ***p*-1-Th** (15.8 mg, 96%) as a yellow solid. ^{1}H NMR ($CDCl_3$): δ 7.62 (dd, J_{HH} = 1.1 Hz, 1.1 Hz, 2H), 7.59 (s, 2H), 7.58 (d, J_{HH} = 0.4 Hz, 2H), 7.34 (dd, J_{HH} = 5.0 Hz, 1.2 Hz, 2H), 7.29 (dd, J_{HH} = 5.1 Hz, 1.2 Hz, 2H), 7.08 (dd, J_{HH} = 5.1 Hz, 3.6 Hz, 2H), 7.05 (s, 2H), 0.54 (s, 6H) ppm. $^{13}C\{^1H\}$ NMR ($CDCl_3$): δ 144.1, 141.8, 136.4, 135.0, 133.4, 133.2, 128.0, 126.8, 125.1, 124.9, 123.4, −4.6. ^{29}Si NMR ($CDCl_3$): δ −11.0 ppm. HRMS (APCI): calcd for $C_{24}H_{21}S_2Si$ [M^+ + H] 401.084845, found 401.084072.

Data for ***m-1-bTh***. The crude product was purified by column chromatography (SiO_2, 5−20% DCM/hexanes) to yield ***m*-1-bTh** (12.6 mg, 43%) as a bright yellow solid. ^{1}H NMR ($CDCl_3$): δ 7.80 (d, J_{HH} = 2.0 Hz, 2H), 7.60 (dd, J_{HH} = 8.1 Hz, 2.0 Hz, 2H), 7.39 (d, J_{HH} = 8.1 Hz, 2H), 7.25 (d, J_{HH} = 3.8 Hz, 2H), 7.22 (dd, J_{HH} = 4.9 Hz, 1.1 Hz, 4H), 7.16 (d, J_{HH} = 3.8 Hz, 2H), 7.04 (dd, J_{HH} = 5.0 Hz, 3.7 Hz, 2H), 6.97 (s, 2H), 0.61 (s, 6H) ppm. $^{13}C\{^1H\}$ NMR ($CDCl_3$): δ 143.0, 140.8, 137.5, 137.4, 137.0, 133.1, 132.8, 130.3, 129.7, 127.9, 126.2, 124.7, 124.4, 123.8, 123.7, −4.7 ppm. ^{29}Si NMR ($CDCl_3$): δ −10.2 ppm. HRMS (APCI): calcd for $C_{32}H_{25}S_4Si$ [M + H^+] 565.060287, found 565.058261.

Data for ***p-1-bTh***. The crude product was purified by column chromatography (SiO_2, 0−20% DCM/hexanes) to yield ***p*-1-bTh** (14.6 mg, 52%) as a yellow solid. ^{1}H NMR ($CDCl_3$): δ 7.60 (d, 2H), 7.58−7.55 (m, 4H), 7.25 (d, J_{HH} = 3.2 Hz, 2H), 7.22 (dd, J_{HH} = 5.2 Hz, 1.2 Hz, 2H), 7.21 (dd, J_{HH} = 3.6 Hz, 2H), 7.15 (d, J_{HH} = 3.6 Hz, 2H), 7.06 (s, 2H), 7.03 (dd, J_{HH} = 5.2 Hz, 3.6 Hz, 2H), 0.54 (s, 6H) ppm. $^{13}C\{^1H\}$ NMR ($CDCl_3$): δ 142.7, 141.9 137.4, 137.0, 136.5, 134.7, 133.4, 133.3, 127.9, 126.4, 124.6, 124.52, 124.5, 124.1, 123.7, −4.6 ppm. ^{29}Si NMR ($CDCl_3$): δ −10.9 ppm. HRMS (EI): calcd for $C_{32}H_{25}S_4Si$ [M + H^+] 565.060287, found 565.060839.

General Procedure for Sonogoshira Coupling Reactions. The Sonogoshira couplings were accomplished using a procedure based on that reported by Buchwald and co-workers.[63] A clean dried two-neck flask was charged with ***m*-1-Cl** or ***p*-1-Br** (0.05 mmol), $PdCl_2(MeCN)_2$ (4 mol %), XPhos (12 mol %), and Cs_2CO_3 (0.93 mmol). Acetonitrile (1 mL) was added and the solution stirred at room temperature for 30 min, after which phenylacetylene (0.91 mmol) was added via syringe and the solution heated to reflux for 36 h. The reaction was cooled to room temperature and filtered over silica, and solvent removed *in vacuo*. The crude product was purified by column chromatography or preparatory GPC.

Data for ***m-1-CCPh***. The crude product was purified by gel permeation chromatography (DCM, 4 mL/min, t_R = 10.71 min) to yield ***m*-1-CCPh** (12.6 mg, 43%) as a bright yellow solid. ^{1}H NMR ($CDCl_3$): δ 7.75 (d, J_{HH} = 1.6 Hz, 2H), 7.58−7.55 (m, 4H), 7.53 (d, J_{HH} = 1.6 Hz, 2H), 7.37−7.35 (m, 8 H), 6.98 (s, 2H), 0.56 (s, 6H) ppm. $^{13}C\{^1H\}$ NMR ($CDCl_3$): δ 140.9, 137.0, 135.8, 133.2, 132.0, 131.6, 129.6, 128.4, 128.3, 123.3, 122.6, 90.8, 89.6, −4.7 ppm. ^{29}Si NMR ($CDCl_3$): δ −10.6 ppm. HRMS (APCI) calcd for $C_{32}H_{25}Si$ [M + H^+]; 437.172004, found 437.172249.

Data for ***p-1-CCPh***. The crude product was purified by column chromatography (SiO_2, 0−10% DCM/hexanes) to yield ***p*-1-CCPh** (10.9 mg, 50%) as a bright yellow solid. ^{1}H NMR ($CDCl_3$): δ 7.56−7.53 (m, 8H), 7.49 (dd, J_{HH} = 7.6 Hz, 1.2 Hz, 2H), 7.36−7.34 (m, 6H), 6.98 (s, 2H), 0.52 (s, 6H) ppm. $^{13}C\{^1H\}$ NMR ($CDCl_3$): δ 141.3, 137.3, 133.1, 132.6, 132.3, 131.6, 130.1, 128.3, 124.0, 123.1, 90.0, 89.1, −4.7 ppm. ^{29}Si NMR ($CDCl_3$): δ −10.4 ppm. HRMS (MALDI): calcd for $C_{32}H_{25}Si$ [M + H^+] 437.1720, found 437.1719.

Synthesis of Mesityl Borepin ***m-2-Ph***. In a glovebox a clean dry round-bottom flask was charged with ***m*-1-Ph** (115 mg, 0.30 mmol) and BBr_3 (2 mL). The dark brown solution was heated in a sealed bomb to 50 °C for 2 days, at which point liquids were removed *in vacuo*. The solids were taken into a glovebox and dissolved in toluene. A suspension of MesLi (76 mg, 0.60 mmol) in toluene (1 mL) was added dropwise, and the suspension stirred for 16 h. Solvent was removed *in vacuo*, and the product purified by column chromatography (SiO_2, 0−15% EtOAc/hexanes). X-ray quality crystals were obtained by recrystallization in toluene/hexanes. ^{1}H NMR ($CDCl_3$): δ 8.32 (d, J_{HH} = 1.2 Hz, 2H), 7.97 (dd, J_{HH} = 8.0 Hz, 2.4 Hz, 2H), 7.89 (dd, J_{HH} = 8.0 Hz, 2H), 7.52−7.49 (m, 4H), 7.43−7.39 (tdd, J_{HH} = 7.4 Hz, 1.2 Hz, 1.2 Hz 4H), 7.41 (s, 2H), 7.32 (tdd, J_{HH} = 7.4 Hz, 2.0 Hz, 1.6 2H), 6.91 (s, 2H), 2.37 (s, 3H), 1.99 (s, 6H) ppm. ^{11}B NMR ($CDCl_3$): δ 43.2 ppm.

■ ASSOCIATED CONTENT

Supporting Information. Synthetic procedures for the tetrahalostilbene starting materials, connectivity structure for ***p*-1-Ph**, full UV−vis and emission spectra for all compounds, including solvatochromism data, HOMO and LUMO surfaces for all compounds, cyclic voltammograms for all compounds, and Cartesian coordinates for computed structures of all compounds. Supplementary crystallographic data for ***m*-1-bTh** (CCDC 801215) and ***m*-2-Ph** (801216) in the form of .cif files. This material is available free of charge via the Internet at http://pubs.acs.org.

■ AUTHOR INFORMATION

Corresponding Author

*Tel: 403-220-5746. Fax: 403-289-9488. E-mail: wpiers@ucalgary.ca.

■ ACKNOWLEDGMENT

This work was supported by the National Science Engineering Research Council of Canada, the Japan Society for the Promotion of Science, Alberta Innovates, the Xerox Research Foundation, and the UK Engineering and Physical Sciences Research Council. We also thank Prof. J. D. Tovar (Johns Hopkins) and co-workers for helpful discussions and disclosure of unpublished work.

■ REFERENCES

(1) Dalton, L. R.; Sullivan, P. A.; Bale, D. H. *Chem. Rev.* **2009**, *110* 25–55.
(2) Mishra, A.; Ma, C.-Q.; Baeuerle, P. *Chem. Rev.* **2009**, *109*, 1141–1276.
(3) Muller, T. J. J.; Bunz, U. H. F., Eds. *Functional Organic Materials*; Wiley-VCH: Weinheim, 2007.
(4) Coropceanu, V.; Cornil, J.; da Silva Filho, D. A.; Olivier, Y.; Silbey, R.; Bredas, J.-L. *Chem. Rev.* **2007**, *107*, 926–952.
(5) Anthony, J. E. *Chem. Rev.* **2006**, *106*, 5028–5048.
(6) Bendikov, M.; Wudl, F.; Perepichka, D. F. *Chem. Rev.* **2004**, *104* 4891–4946.
(7) Ponomarenko, S.; Kirchmeyer, S. Conjugated Organosilicon Materials for Organic Electronics and Photonics. In *Silicon Polymers*; Muzafarov, A. M., Ed.; Springer: Berlin, 2011; Vol. 235, pp 33−110.
(8) Yamaguchi, S.; Tamao, K. *J. Chem, Soc., Dalton Trans.* **1998**, 3693–3702.
(9) Yamaguchi, S.; Endo, T.; Uchida, M.; Izumizawa, T.; Furukawa, K.; Tamao, K. *Chem.—Eur. J.* **2000**, *6*, 1683–1692.
(10) Tang, B. Z.; Zhan, X.; Yu, G.; Lee, P. P. S.; Liu, Y.; Zhu, D. *J. Mater. Chem.* **2001**, *11*, 2974–2978.
(11) Uchida, M.; Izumizawa, T.; Nakano, T.; Yamaguchi, S.; Tamao, K.; Furukawa, K. *Chem. Mater.* **2001**, *13*, 2680–2683.
(12) Chen, J.; Law, C. C. W.; Lam, J. W. Y.; Dong, Y.; Lo, S. M. F.; Williams, I. D.; Zhu, D.; Tang, B. Z. *Chem. Mater.* **2003**, *15*, 1535–1546.
(13) Boydston, A. J.; Yin, Y.; Pagenkopf Brian, L. *J. Am. Chem. Soc.* **2004**, *126*, 3724–5.
(14) Lee, K.-H.; Ohshita, J.; Kunai, A. *Organometallics* **2004**, *23* 5481–5487.
(15) Ohshita, J.; Lee, K.-H.; Hamamoto, D.; Kunugi, Y.; Ikadai, J.; Kwak, Y.-W.; Kunai, A. *Chem. Lett.* **2004**, *33*, 892–893.
(16) Yamaguchi, S.; Xu, C.; Yamada, H.; Wakamiya, A. *J. Organomet. Chem.* **2005**, *690*, 5365–5377.
(17) Zhan, X.; Risko, C.; Amy, F.; Chan, C.; Zhao, W.; Barlow, S.; Kahn, A.; Bredas, J.-L.; Marder, S. R. *J. Am. Chem. Soc.* **2005**, *127*, 9021–9029.
(18) Geramita, K.; McBee, J.; Shen, Y.; Radu, N.; Tilley, T. D. *Chem. Mater.* **2006**, *18*, 3261–3269.
(19) Usta, H.; Lu, G.; Facchetti, A.; Marks, T. J. *J. Am. Chem. Soc.* **2006**, *128*, 9034–9035.
(20) Karle, I. L.; Butcher, R. J.; Wolak, M. A.; da Silva Filho, D. A.; Uchida, M.; Bredas, J.-L.; Kafafi, Z. H. *J. Phys. Chem. C* **2007**, *111*, 9543–9547.
(21) Li, L.; Xiang, J.; Xu, C. *Org. Lett.* **2007**, *9*, 4877–4879.
(22) Zhan, X.; Haldi, A.; Risko, C.; Chan, C. K.; Zhao, W.; Timofeeva, T. V.; Korlyukov, A.; Antipin, M. Y.; Montgomery, S.; Thompson, E.; An, Z.; Domercq, B.; Barlow, S.; Kahn, A.; Kippelen, B.; Bredas, J.-L.; Marder, S. R. *J. Mater. Chem.* **2008**, *18*, 3157–3166.
(23) Furukawa, S.; Kobayashi, J.; Kawashima, T. *J. Am. Chem. Soc.* **2009**, *131*, 14192–14193.
(24) Wong, W. W. H.; Hooper, J. F.; Holmes, A. B. *Aust. J. Chem.* **2009**, *62*, 393–401.
(25) Zhan, X.; Barlow, S.; Marder, S. R. *Chem. Commun.* **2009** 1948–1955.
(26) Li, L.; Xu, C.; Li, S. *Tetrahedron Lett.* **2010**, *51*, 622–624.
(27) Yamaguchi, S.; Tamao, K. *Bull. Chem. Soc. Jpn.* **1996**, *69*, 2327–2334.
(28) Maier, G.; Mihm, G.; Reisenauer, H. P. *Angew. Chem., Int. Ed. Engl.* **1980**, *19*, 52–53.
(29) Solouki, B.; Rosmus, P.; Bock, H.; Maier, G. *Angew. Chem., Int. Ed. Engl.* **1980**, *19*, 51–52.
(30) Tanabe, Y.; Mizuhata, Y.; Tokitoh, N. *Organometallics* **2010**, *29*, 721–723.
(31) Tokitoh, N.; Shinohara, A.; Matsumoto, T.; Sasamori, T.; Takeda, N.; Furukawa, Y. *Organometallics* **2007**, *26*, 4048–4053.
(32) Shinohara, A.; Takeda, N.; Sasamori, T.; Tokitoh, N. *Bull. Chem. Soc. Jpn.* **2005**, *78*, 977–987.
(33) Tokitoh, N. *Acc. Chem. Res.* **2004**, *37*, 86–94.
(34) Takeda, N.; Shinohara, A.; Tokitoh, N. *Organometallics* **2002**, *21*, 256–258.
(35) Takeda, N.; Shinohara, A.; Tokitoh, N. *Organometallics* **2002**, *21*, 4024–4026.
(36) Wakita, K.; Tokitoh, N.; Okazaki, R.; Takagi, N.; Nagase, S. *J. Am. Chem. Soc.* **2000**, *122*, 5648–5649.
(37) Wakita, K.; Tokitoh, N.; Okazaki, R.; Nagase, S.; Schleyer, P. v. R.; Jiao, H. *J. Am. Chem. Soc.* **1999**, *121*, 11336–11344.
(38) Tokitoh, N.; Wakita, K.; Okazaki, R.; Nagase, S.; Schleyer, P. v. R.; Jiao, H. *J. Am. Chem. Soc.* **1997**, *119*, 6951–6952.
(39) Corey, J. Y.; Dueber, M.; Bichlmeir, B. *J. Organomet. Chem.* **1971**, *26*, 167–173.
(40) Barton, T. J.; Volz, W. E.; Johnson, J. L. *J. Org. Chem.* **1971**, *36*, 3365–3367.
(41) Cartledge, F. K; Mollere, P. D. *J. Organomet. Chem.* **1971**, *26*, 175–181.
(42) Corey, J. Y.; Corey, E. R. *Tetrahedron Lett.* **1972**, 4669.
(43) Barton, T. J.; Kippenha, R. C.; Nelson, A. J. *J. Am. Chem. Soc.* **1974**, *96*, 2272–2273.
(44) Barton, T. J.; Kippenha, R. C.; Nelson, A. J. *J. Am. Chem. Soc.* **1974**, *96*, 2272–2273.
(45) Corey, E. R.; Corey, J. Y.; Glick, M. D. *J. Organomet. Chem.* **1975**, *101*, 177–186.
(46) Corey, E. R.; Corey, J. Y.; Glick, M. D. *J. Organomet. Chem.* **1977** *129*, 17–25.
(47) Lange, L. D.; Corey, J. Y.; Rath, N. P. *Organometallics* **1991**, *10*, 3189–3196.
(48) Sakamoto, H.; Ishikawa, M. *J. Organomet. Chem.* **1991**, *418* 305–309.
(49) Corey, J. Y.; Pitts, A. J.; Winter, R. E. K.; Rath, N. P. *J. Organomet. Chem.* **1995**, *499*, 113–121.
(50) Nishinaga, T.; Izukawa, Y.; Komatsu, K. *J. Phys. Org. Chem.* **1998**, *11*, 475–477.
(51) Nishinaga, T.; Izukawa, Y.; Komatsu, K. *Chem. Lett.* **1998**, 269–270.
(52) Nishinaga, T.; Izukawa, Y.; Komatsu, K. *Tetrahedron* **2001**, *57* 3645–3656.
(53) Kira, M.; Ishida, S.; Iwamoto, T.; Kabuto, C. *J. Am. Chem. Soc.* **2002**, *124*, 3830–3831.
(54) Shirani, H.; Janosik, T. *Organometallics* **2008**, *27*, 3960–3963.
(55) Nakadaira, Y.; Sato, R.; Sakurai, H. *Organometallics* **1991**, *10* 435–442.
(56) Corey, J. Y.; Trankler, K. A.; Braddock-Wilking, J.; Rath, N. P. *Organometallics* **2010**, *29*, 5708–5713.
(57) Mercier, L. G.; Piers, W. E.; Parvez, M. *Angew. Chem., Int. Ed.* **2009**, *48*, 6108–6111.
(58) Caruso, A.; Siegler, M. A.; Tovar, J. D. *Angew. Chem., Int. Ed.* **2010**, *49*, 4213–4217.
(59) Caruso, A.; Tovar, J. D. *J. Org. Chem.* **2011**, DOI: 10.1021/jo2001726.
(60) Krasovskiy, A.; Knochel, P. *Angew. Chem., Int. Ed.* **2004**, *43*, 3333–3336.
(61) Wolfe, J. P.; Buchwald, S. L. *Angew. Chem., Int. Ed.* **1999**, *38* 2413–2416.
(62) Littke, A. F.; Schwarz, L.; Fu, G. C. *J. Am. Chem. Soc.* **2002**, *124* 6343–6348.

(63) Gelman, D.; Buchwald, S. L. *Angew. Chem., Int. Ed.* **2003**, *42* 5993–5996.
(64) See the Supporting Information for the UV−vis and emission spectra of all the new compounds described herein.
(65) Lippert, V. E. *Z. Electrochem.* **1957**, *61*, 962.
(66) Mataga, N.; Kaifu, Y.; Koizumi, M. *Bull. Chem. Soc. Jpn.* **1956**, *29*, 465.
(67) Job, A.; Wakamiya, A.; Kehr, G.; Erker, G.; Yamaguchi, S. *Org. Lett.* **2010**, *12*, 5470–5473.
(68) Wood, T. K.; Piers, W. E.; Keay, B. A.; Parvez, M. *Angew. Chem., Int. Ed.* **2009**, *48*, 4009–4012.
(69) Song, C.; Swager, T. M. *J. Org. Chem.* **2009**, *75*, 999–1005.
(70) See the Supporting Information for the full citation.